

RESEARCH ARTICLE

Open Access



Automatic measurement of lower limb alignment in portable devices based on deep learning for knee osteoarthritis

Jianfeng Yang^{1,2†}, Peng Ren^{2†}, Peng Xin^{3†} , Yiming Wang^{1,2,4}, Yonglei Ma⁵, Wei Liu⁶, Yu Wang⁶, Yan Wang^{1,2,7*} and Guoqiang Zhang^{1,2,7,8*}

Abstract

Background For knee osteoarthritis patients, analyzing alignment of lower limbs is essential for therapy, which is currently measured from standing long-leg radiographs of anteroposterior X-ray (LLR) manually. To address the time wasting, poor reproducibility and inconvenience of use caused by existing methods, we present an automated measurement model in portable devices for assessing knee alignment from LLRs.

Method We created a model and trained it with 837 conforming LLRs, and tested it using 204 LLRs without duplicates in a portable device. Both manual and model measurements were conducted independently, then we recorded knee alignment parameters such as Hip knee ankle angle (HKA), Joint line convergence angle (JCLA), Anatomical mechanical angle (AMA), mechanical Lateral distal femoral angle (mLDFA), mechanical Medial proximal tibial angle (mMPTA), and the time required. We evaluated the model's performance compared with manual results in various metrics.

Result In both the validation and test sets, the average mean radial errors were 2.778 and 2.447 ($P < 0.05$). The test results for native knee joints showed that 92.22%, 79.38%, 87.94%, 79.82%, and 80.16% of the joints reached angle deviation $< 1^\circ$ for HKA, JCLA, AMA, mLDFA, and mMPTA. Additionally, for joints with prostheses, 90.14%, 93.66%, 86.62%, 83.80%, and 85.92% of the joints reached that. The Chi-square test did not reveal any significant differences between the manual and model measurements in subgroups ($P > 0.05$). Furthermore, the Bland-Altman 95% limits of agreement were less than $\pm 2^\circ$ for HKA, JCLA, AMA, and mLDFA, and slightly more than ± 2 degrees for mMPTA.

Conclusion The automatic measurement tool can assess the alignment of lower limbs in portable devices for knee osteoarthritis patients. The results are reliable, reproducible, and time-saving.

Keywords Knee osteoarthritis, Deep learning, Lower limb alignment, Total knee arthroplasty

[†]Jianfeng Yang, Peng Ren and Peng Xin contributed equally to this work.

*Correspondence:

Yan Wang
yanwang_plagh@163.com
Guoqiang Zhang
gqzhang_plagh@163.com

Full list of author information is available at the end of the article



© The Author(s) 2024. **Open Access** This article is licensed under a Creative Commons Attribution 4.0 International License, which permits use, sharing, adaptation, distribution and reproduction in any medium or format, as long as you give appropriate credit to the original author(s) and the source, provide a link to the Creative Commons licence, and indicate if changes were made. The images or other third party material in this article are included in the article's Creative Commons licence, unless indicated otherwise in a credit line to the material. If material is not included in the article's Creative Commons licence and your intended use is not permitted by statutory regulation or exceeds the permitted use, you will need to obtain permission directly from the copyright holder. To view a copy of this licence, visit <http://creativecommons.org/licenses/by/4.0/>. The Creative Commons Public Domain Dedication waiver (<http://creativecommons.org/publicdomain/zero/1.0/>) applies to the data made available in this article, unless otherwise stated in a credit line to the data.

Introduction

Knee osteoarthritis (knee OA), can cause significant joint pain, decreased mobility, and even disability [1]. For patients in the end stage of the condition, Total Knee Arthroplasty (TKA) is a commonly used and highly effective therapy [2]. It is important to properly assess alignment during the perioperative period to ensure optimal outcomes [3]. Lower limb alignment is a critical aspect that surgeons carefully evaluate when assessing deformity, predicting treatment outcomes, and planning for surgery. For cases involving knee OA, the majority of surgeons agree that achieving a neutrally aligned lower limb after TKA is a crucial objective [4].

Long-leg radiographs of anteroposterior X-ray (LLR) quantify alignment by identifying specific anatomic landmarks [5, 6]. Long-leg radiographs of anteroposterior X-ray (LLR) quantify alignment by identifying specific anatomic landmarks [7]. Currently, surgeons measure alignment using standard rulers, digital calipers, or manual measurements in hospital computer systems like PACS (Picture Archiving and Communication System) [8]. LLR is considered the gold standard for radiological imaging of lower limbs in weight-bearing standing positions, providing insight into their mechanics [5, 6]. However, manual methods for measuring the tibial-femoral angle have drawbacks such as being time-consuming, inconvenient, and having low reproducibility of results. Additionally, the reliability of these methods relies on clinical experience. To address these issues, Takahashi et al. [9] proposed a self-developed method that uses digital technology to measure the angle on a radiographic film. This method requires the observer to identify four standardized points using a mouse and calculate the angle. Sled et al. [10] proposed a landmark-based method for assessing Hip knee ankle angle (HKA) using customized software, addressing common issues in similar methods. In clinical practice, measurement accuracy can be influenced by factors such as body position [11–13] (like loading, flexion, or rotation of lower limbs), image quality [7], and reader experience [14–16]. Even with software assistance, deviations caused by hardware facilities and use can also affect the measurement, which leads to inter- and intra-reader variability and unsatisfied reliability [17–19]. In actual use, landmarks selection manually can also be time-consuming.

With the advancements in Artificial Intelligence, Deep Learning-based image analysis is increasingly being utilized in clinical medicine. As the volume of imaging data grows, AI-powered software can provide high-quality assessment outputs in less time and with reduced effort required from surgeons. Simon et al [3] proposed a fully automated deep learning tool based on the LAMA model for knee alignment assessment and limb length measurements. Tack et al [20] proposed a similar fully automated

tool for measuring the HKA from LLR based on YOLOv4 And Resnet Landmark regression Algorithm. According to the researchers, their tools based on various models have achieved satisfactory accuracy. But, Tack et al's tool only identifies the knee as varus or valgus deformity through HKA, and Simon et al's model cannot assess lower extremity alignment after TKA. Moreover, there is no diagnostic tool for clinical use resulting from most of the current studies.

For this study, we analyzed the average angle measurements of up to 3 orthopedic surgeons for each LLR and compared them to the results generated by a fully automated tool. The tool was specifically trained to provide clinically significant angles of alignment, both with and without the presence of a prosthesis in LLRs.

Materials and methods

This study was approved by the Ethics Review Board of the First Medical Center of Chinese PLA General Hospital.

We retrospectively reviewed 1041 digital LLR X-rays (from 623 patients) in the dataset of the General Hospital of the People's Liberation Army. These X-rays were captured using the uDR 780i Pro Fully Automatic Ceiling-mounted DR (UNITED IMAGING, Shanghai, China) between January and December 2021. Each patient may have undergone multiple pre- and post-operative radiographs. All X-rays were performed for clinical or perioperative measurements.

The inclusion criteria were as follows: (1) patient age ≥ 40 ; (2) knee OA diagnosis established based on the Chinese Guidelines for the Diagnosis and Treatment of Osteoarthritis (2019 edition) [21]; (3) standing LLR X-rays of both lower limbs; (4) for the same patient, over 90 days between examinations; (5) previous total knee arthroplasty history or no surgery history. The exclusion criteria were as follows: (1) non-standard standing LLR X-rays; (2) severe deformity of the femur or tibia; (3) comorbidities of other diseases that may cause severe knee deformities or joint fusion; (4) comorbidities including infectious arthritis or postoperative joint infection; (5) LLRs showing other implants like uni-compartmental knee prosthesis or internal fixation; (6) incorrect posture (such as rotation or flexion of lower limbs); (7) poor image quality.

Model architecture

We divide the included LLRs into a training set (837), a validation set (101), and a test set (204) according to approximately 80%:10%:20%. For the training set (LLRs were stored with an average size of 2021×2021 and a pixel spacing of 0.2 mm), these were calibrated landmarks by orthopaedic specialists, which was implemented in MATLAB (Mathworks, Natick, MA). Then all

images were resized to 640×320 pixels with the isotropic spacing of 0.79 mm using a bilinear interpolation algorithm and then normalized for model development.

As Liu et al. [22] demonstrated in their study about preoperative planning of total hip arthroplasty, we formulated the alignment measurement to a task including two branches: (1) landmarks detection branch, and (2) edges prediction branch. Each resized LLR was firstly input into the backbone network to extract high-level features for two branches.

As for the backbone network, we used the HRNet model for 2 branches above (the proposed model is shown in Fig. 1) [23]. For landmarks detection, each landmark was converted into a heatmap with a 2D Gaussian distribution centered at its coordinates (the hyperparameter σ of Gaussian heatmaps is chosen to be 2), and the distribution is normalized to $[0,1]$. For edge prediction, each edge connecting two landmarks was denoted as a vector and normalized during the experiment for faster convergence, which was a constraint for helping correct the detection deviations implicitly during training.

The proposed model was implemented using PyTorch and ran on a machine with 4 Nvidia P100 GPUs. The parameters of the network were initialized with the pre-trained model from the large public dataset ImageNet [24]. In addition, the training set was augmented by several methods commonly used [25]. According to the study of Adam [26], the backbone network was optimized with an initial learning rate of $1e-3$, which was decreased to $1e-4$ and $1e-5$ at the 120th and 170th epochs. During

the model development, the training loss curve normally decreased and stabilized without overfitting. The overall optimization is carried out for 200 epochs with a batch size of 32.

Surgeons' evaluation

To test the accuracy of the tool, We used 204 images as a training set from knee OA patients who had not undergone surgery, and those who had undergone unilateral or bilateral total knee replacement surgery (Some patients may have multiple images pre- and post-operatively). There was no duplication of the test set with either the training or validation sets. To assess the measurements of the proposed model, after removing patient information, each LLR was measured by two senior surgeons on a blinded basis independently in PACS, including HKA, JCLA (Joint line convergence angle), AMA (Anatomical mechanical angle), mL DFA (mechanical Lateral distal femoral angle), and mMPTA (mechanical Medial proximal tibial angle). They accomplished this by manually identifying and connecting the corresponding landmarks. The average of the measurements for the landmarks and angles of alignment were considered to be the ground truths. In the portable device, all LLRs were captured using mobile phones (iPhone X, Apple Inc.). During the photo session, the phone was mounted on a tripod, positioned 40 cm away from the LLRs, and centered with them for constant indoor lighting. The images were saved in JPG format and had a resolution of 4000×3000 pixels. These images were not optimized or pre-processed

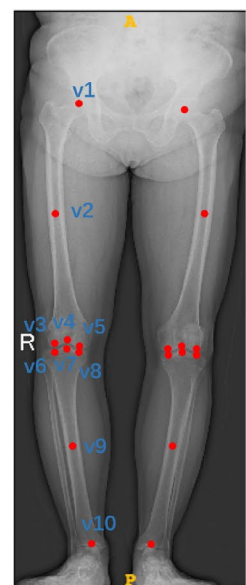
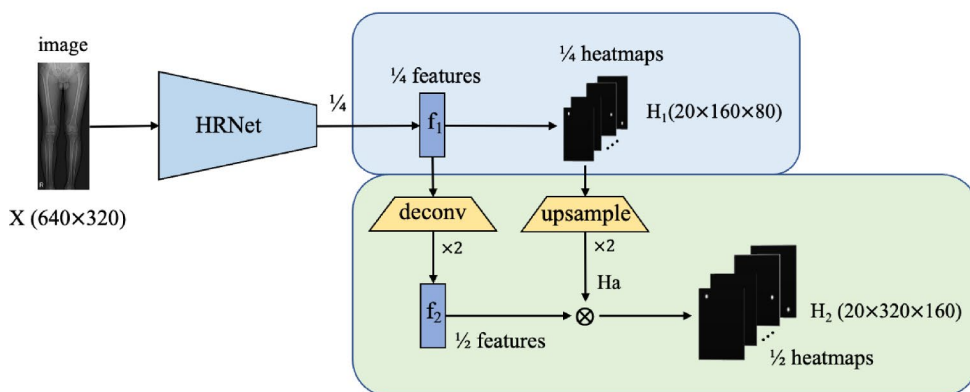


Fig. 1 The framework of the proposed method and examples of corresponding landmarks. v1, Centre of the femoral head; v2, Centre of the femoral diaphysis; v3, Lowest point of lateral femoral condyle or prosthesis; v4, Centre of the knee joint or prosthesis on the femoral side; v5, Lowest point of medial femoral condyle or prosthesis; v6, Lowest point of lateral tibial plateau or prosthesis; v7, Centre of the knee joint or prosthesis on the tibia side; v8, Lowest point of medial tibial plateau or prosthesis; v9, Centre of the tibia diaphysis; v10, Centre of the ankle joint. LLR was from a 65-year-old female patient diagnosed with knee OA and authorized consent was obtained from the patient before the use

Table 1 The MRE for landmark and average in the validation and test sets

Landmarks Datasets	V1	V2	V3	V4	V5	V6	V7	V8	V9	V10	mean
Validation set	5.432	4.429	2.266	1.514	2.226	2.547	2.081	2.325	3.223	1.740	2.778
Test set	4.131	2.978	2.272	1.508	2.233	2.395	2.012	2.309	3.105	1.528	2.447

Table 2 Demographics and morphological data in test set

Variables	Test set (n = 408 knee joints) n (%) or Mean ± SD (Range)
Native Knee Joint	262
number of detected†	257 (98.1%)
number of undetected†	5 (1.9%)
sex(female/male)	115/39
age(year)*	62.72 ± 8.16
BMI*	25.98 ± 3.33
side(left/right)†	133 (51.8%)/124 (48.2%)
K-L grade†	
K-L 2	25 (9.7%)
K-L 3	107 (41.6%)
K-L 4	125 (48.6%)
length of symptoms†	
<5 years	58 (22.6%)
5–10 years	119 (46.3%)
>10 years	80 (31.1%)
alignment status†	
varus	140 (54.5%)
neutral	79 (30.7%)
valgus	38 (14.8%)
Joint with Prosthesis	146
number of detected†	142 (97.3%)
number of undetected†	4 (2.7%)
sex(female/male)	73/29
age(year)*	65.33 ± 5.11
BMI*	27.32 ± 3.47
side(left/right)†	63 (44.4%)/79 (55.6%)

*the values are given as the mean and standard deviation;

†the values are given as the number with the percentage in parentheses

before being fed into the model, and the model output the predictions.

Statistical analysis

To compare the performance of landmarks detection, we adopted mean radial error (MRE) for quantitative comparison, which was defined as

$$MRE = 1/n \sum_{i=1}^n R_i$$

n denoted the number of detected landmarks and *R_i* was the Euclidean distance between the predicted landmarks coordinates obtained by extracting the maxima on heatmaps and the ground truths. To assess the results of the proposed model, we adopted the Chi-Square test. *P* ≥ 0.05 was considered to represent no significant

Table 3 Correlations and agreement of manual and automatic measurements of alignment and used time

	Knee Joint†	MAD*	% AD<1°†	% AD<2°†	P value
Native Joint					
HKA	257	0.47 ± 0.38	92.22%	99.20%	
JCLA	257	0.65 ± 0.60	79.38%	96.50%	
AMA	257	0.48 ± 0.44	87.94%	99.22%	
mMPTA	257	0.79 ± 0.87	79.82%	93.39%	
mLDFA	257	0.62 ± 0.54	80.16%	97.67%	
Used time*					<0.01
mean manual		173.78 ± 12.37			
model		2.53 ± 0.80			
Joint with Prosthesis					
HKA	142	0.51 ± 0.40	90.14%	98.59%	
JCLA	142	0.34 ± 0.38	93.66%	98.59%	
AMA	142	0.50 ± 0.43	86.62%	99.30%	
mMPTA	142	0.55 ± 0.46	83.80%	98.59%	
mLDFA	142	0.54 ± 0.42	85.92%	99.30%	
Used time*					<0.01
mean manual		175.04 ± 13.11			
model		2.54 ± 0.80			

MAD, mean absolute difference

AD, average deviation

*the values are given as the mean and standard deviation;

†the values are given as the number with the percentage in parentheses

difference between manual measurements and model calculations. Bland-Altman was adopted to assess the consistency between the two methods. For angles, previous studies considered a difference of >2° as clinically relevant [3], so we adopted >1° and >2° respectively. The data were analyzed using R (4.0.0) and SPSS Version 25.0.0.2 (SPSS, Inc., Chicago, Ill.).

Result

For comparing the results of the validation and test sets, the average of MREs were 2.778 and 2.447 between the two datasets, and MREs of each landmark were listed in Table 1. For both the model and the clinical use, each side of the lower limb was measured separately. In the test set, 204 images from 167 patients were included (the demographics and morphological data were shown in Table 2), 98.09% (257 of 262) of those with a native knee joint were identified, and 97.26% (142 of 146) of those with a prosthesis identified (as shown in Table 3).

The automatic measurement results were highly correlated with the standard reference [27]. with the mean

Table 4 Accuracy/inaccuracy and Chi-square test of HKA in test set

	Native Joint		χ^2	p value	Joint with Prosthesis		χ^2	p value
	accuracy	inaccuracy			accuracy	inaccuracy		
Alignment status								
Varus ($\leq -2^\circ$)	179	14	0.975	0.614	72	6	3.511	0.173
Neutural ($-2^\circ \sim +2^\circ$)	38	3			47	5		
Valgus ($\geq 2^\circ$)	20	3			9	3		
Sex								
Male	50	8	3.771	0.052	30	5	1.024	0.312
Female	187	12			98	9		
BMI								
BMI ≤ 25	68	5	0.552	0.458	32	5	0.752	0.386
BMI > 25	166	18			96	9		
Age								
age ≤ 60	52	5	0.537	0.464	28	3	0.001	0.969
age > 60	187	12			100	11		

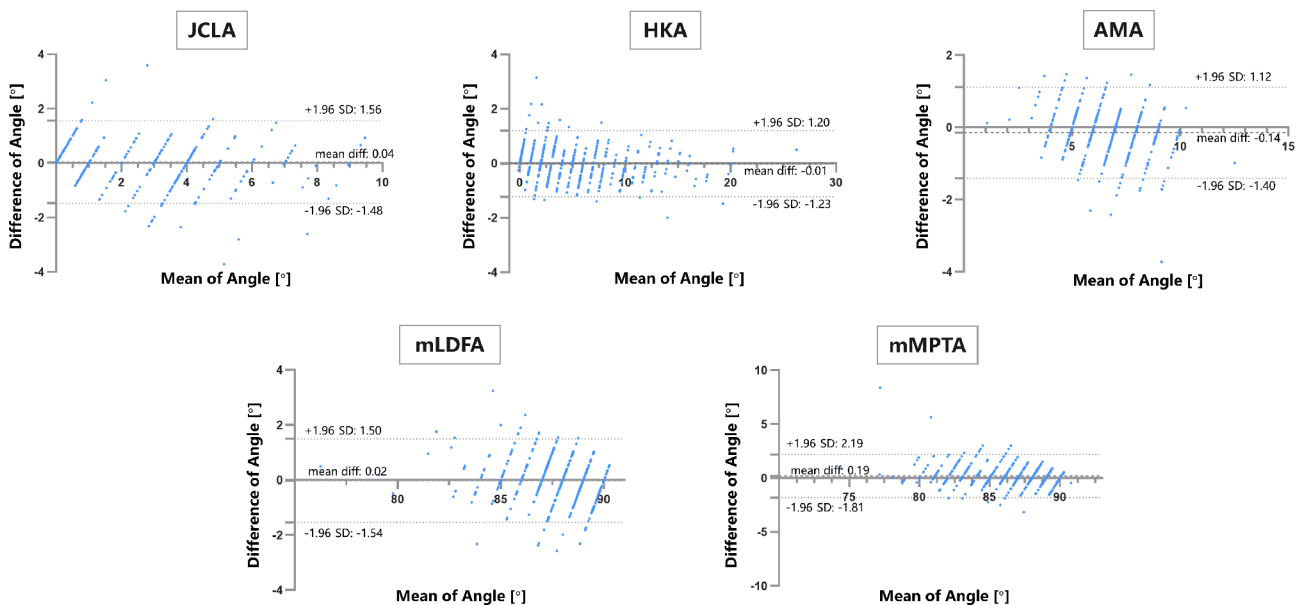


Fig. 2 Comparative evaluation of manual and automatic measurement of lower limb alignment. Bland-Altman plots display the agreement between both surgeons' manual reference and model measurements. diff, difference; SD, standard deviation

absolute difference (MAD) of HKA, JCLA, AMA, mMP TA, mL DFA, being, respectively, 0.47 ± 0.38 , 0.65 ± 0.60 , 0.48 ± 0.44 , 0.79 ± 0.87 , 0.62 ± 0.54 for the lower limbs with a native knee joint and 0.51 ± 0.40 , 0.34 ± 0.38 , 0.50 ± 0.43 , 0.55 ± 0.46 , 0.54 ± 0.42 for lower limbs with a prosthesis. And the percentage of angle deviation (AD) $< 1^\circ$ of HKA, JCLA, AMA, mMP TA, mL DFA, achieved 92.22%, 79.38%, 87.94%, 79.82%, 80.16% for those with a native knee joint and 90.14%, 93.66%, 86.62%, 83.80%, 85.92% for those with a prosthesis respectively. Automated measurement saved over 98% of the time compared to manual methods.

In order to assess whether the measurements were affected by patient characteristics, we classified the test set according to alignment status, sex, BMI, and age (as

shown in Table 4). The accuracy was defined as $AD < 1^\circ$. And after we regrouping the patients in the test set according to those, The Chi-square test for HKA showed no significant differences between the model and manual measures in subgroups ($P > 0.05$ for each subgroup).

The average of manual measurements was considered as ground truth. Bland-Altman plots showed the consistency between prediction angle and ground truth (as shown in Fig. 2). In the Bland-Altman plots, the dashed line denoted the mean of the difference between the two methods that value is -0.014, 0.039, -0.144, 0.187, -0.023 for HKA, JCLA, AMA, mMP TA, mL DFA respectively. And the dotted lines denoted ± 1.96 standard deviations that value was away from the mean of difference. Bland-Altman plots showed that 95% limits of agreement were

1.200 and -1.227, 1.557 and -1.479, 1.116 and -1.404, 2.191 and -1.814, 1.497 and -1.54 for HKA, JCLA, AMA, mL DFA respectively.

Discussion

In this study, for knee OA patients, we presented a fully automated model in portable devices for measuring the alignment of the lower extremity and validated its consistency with surgeons’ measurements. We took five indicators of HKA, JCLA, AMA, mL DFA, mMP TA. The images were taken directly from the portable device without any need for pre-processing. The MRE findings from both the validation and test sets indicate the model’s exceptional generalization and robustness. Additionally, the Bland-Altman analysis demonstrated that the model’s measurements were reliable, whether or not the images had knee prostheses.

According to Table 3, stricter measurement criteria with AD<1° yield lower percentage outcomes for JCLA (79.38%), mMP TA (79.82%), and mL DFA (80.16%), especially for native knee joints. This is primarily because knee OA patients may have varying levels of abrasion and osteophytes present on the tibiofemoral joint surface, causing corresponding landmarks to be dense and indistinct. As a result, there may be a potential discrepancy in anatomical locations (landmarks) detection between manual and model measurements, due to slight variations in practice. As the prosthesis appeared clearly on LLRs, made it easier to identify landmarks during manual measurements. Compared to natural knees, knee joints with prostheses exhibit lower measurement differences (MAD and AD<1°) in JCLA, mMP TA, and mL DFA. Additionally, during the manual examination, surgeons usually zoom in on the femoral condyles and

tibial plateau to detect landmarks in images, but the model was able to directly detect all landmarks in the images. Such differences in practice may also affect measurement consistency. Tables 2 and 4 show that the test set patients were more likely to be women, overweight or obese, older, and have lower limb varus deformity. This is consistent with knee OA disease progression and what we have observed in the clinic.

In research concerning lower limb alignment, multiple measurements are commonly taken by researchers in order to reduce errors [3, 20, 28, 29]. The previous study showed that knee OA patients had a broader distribution of lower limb alignment, making manual measurement more difficult, especially in large patient cohorts for research [27, 28]. In this context, with the development of deep learning, fully automated measurement improves diagnostic accuracy and reproducibility, benefiting related clinical work and research (the actual use of the process is illustrated in Fig. 3). Deep learning is typically used for segmentation, detection, or classification tasks, however, for achieving angle measurements, it is necessary to adapt the complex post-processing of images [30]. In conventional manual measurement techniques, alignments were determined by specifying specific anatomical locations on the limb and then measuring the angle of the connection between the points. Building on this, the proposed model adopted a similar logical approach based on automatic landmark detection and produced accurate and reliable measurement results across a wide range of morphological configurations.

Similar studies have yielded close results for alignment measurements of lower-extremity [3, 20, 30]. Compared to these, we saved more time and achieved automated measurements on portable devices, which greatly

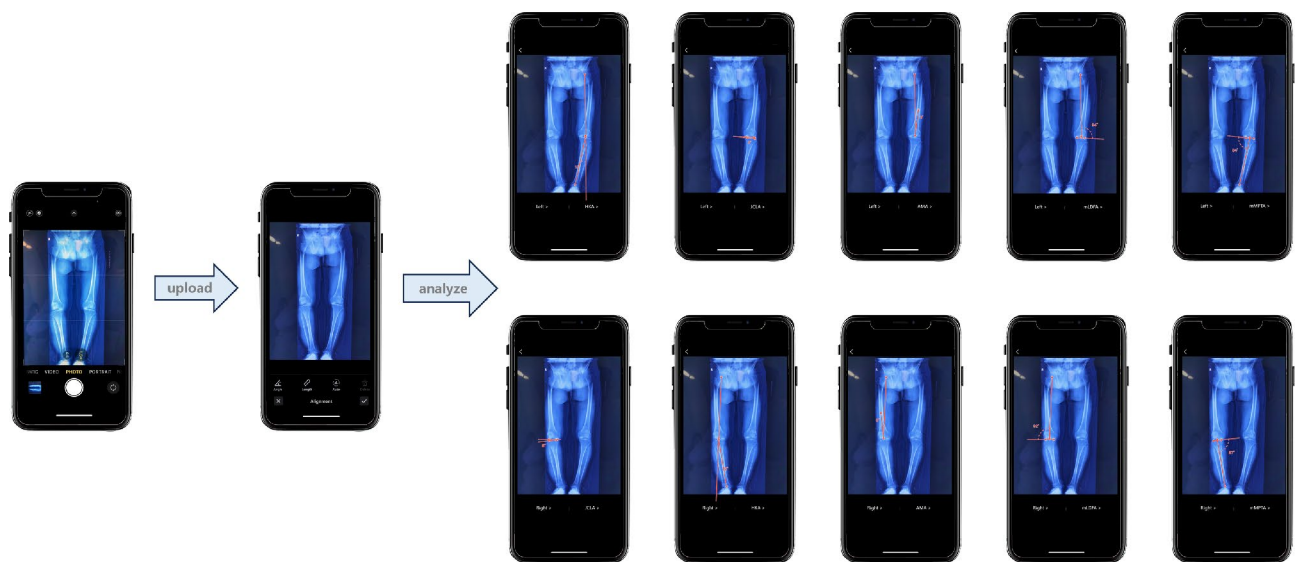
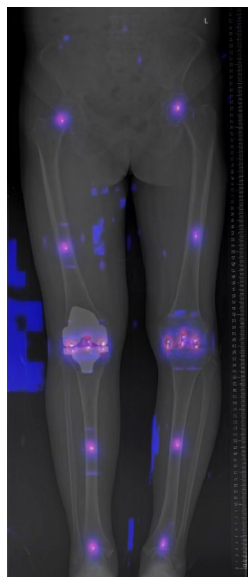


Fig. 3 Actual use of the measuring tool schematic in portable device

Fig. 4 Examples of landmarks detection in the heatmap. LLR was from a 67-year-old female patient diagnosed with knee OA after unilateral TKA and authorized consent was obtained from the patient before the use



facilitates practical use. The HRNet model, proposed for visual recognition problems in 2D images, was adopted in our study [23]. Compared to existing low-resolution classification networks or high-resolution representational learning networks, HRNet was characterised by the following features: it connected high- and low-resolution convolutions in parallel; it maintained high resolution throughout the process, rather than recovering high resolution from low resolution; it repeatedly fused multi-resolution representations, producing rich high-resolution representations with strong positional sensitivity; its storage cost was comparable to available technologies [4]. These features allowed us to guarantee accurate measurements while allowing the model to run on portable devices.

This study had limitations. First, unilateral LLRs were excluded for methodological consistency, which limited the diversity of the data to some extent. Second, as knee OA is a chronic degenerative disease, the entire data set was skewed towards middle-aged and older people. The efficacy of this model needs further investigation to assess the fit in younger knee OA patients or non-knee OA patients. Thirdly, knee OA or post-TKA patients were included. Therefore, the accuracy of the model measurements also needed to be further investigated in post-unicompartamental knee arthroplasty or post-internal fixation of the lower limb patients. Fourth, in patients with severe femoral or tibial deformities, traditional alignment assessment methods were not applicable and were not suitable for automated measurement. Fifth, there were still images that could not be identified, requiring further improvements to the model and more explicit requirements for the quality of the LLRs (Fig. 4).

Conclusion

The deep learning-based measurement tool can be used to assess the lower-limbs alignment of knee OA patients in portable devices. The results are highly reliable, reproducible, and time-saving.

Abbreviations

knee OA	knee osteoarthritis
TKA	total knee arthroplasty
LLR	long-leg radiograph of anteroposterior X-ray
PACS	Picture Archiving and Communication System
HKA	Hip knee ankle angle
JCLA	Joint line convergence angle
AMA	Anatomical mechanical angle
mLDFA	mechanical Lateral distal femoral angle
mMPTA	mechanical Medial proximal tibial angle
MRE	mean radial error
MAD	mean absolute difference
AD	angle deviation
SD	standard deviation
BMI	body mass index

Acknowledgements

The authors thank all staff from the participating departments and clinics.

Author contributions

JY, PR, and PX designed the study and wrote the article. JY, YM, and PX participated in the analysis of the data and contributed to the interpretation of the results. WL, JY, and YW proposed the model. YW and GQZ provided guidance on the design of the study and revised the article. YW and GQZ are mainly responsible for this project. All authors read and approved the final manuscript.

Funding

This study was not supported by any funding.

Data availability

The datasets used and/or analyzed during the current study are available from the corresponding author upon reasonable request.

Declarations

Ethics approval and consent to participate

This study was performed in accordance with the ethical standards in the 1964 Declaration of Helsinki. Permission to waive the informed consent was obtained from the institutional review board (the First Medical Center of Chinese People's Liberation Army General Hospital) for this study. Informed consent was obtained from all individual participants included in the study.

Consent for publication

We have obtained consent to publish from the participants.

Conflict of interest

Each author certifies that he or she has no commercial associations.

Competing interests

The authors declare no competing interests.

Author details

¹Department of Orthopedics, the First Medical Center of Chinese PLA General Hospital, Beijing, China

²Senior Department of Orthopedics, the Fourth Medical Center of Chinese PLA General Hospital, Beijing, China

³Department of Orthopedics, Chinese PLA Southern Theater Command General Hospital, Guangzhou, China

⁴Medical School of Chinese People's Liberation Army, Beijing, China

⁵Department of Anesthesiology, Guangzhou First People's Hospital, Guangzhou, China

⁶Damo Academy, Alibaba Group, Hangzhou, China

⁷Department of Orthopedics, the First Medical Center, PLA General Hospital, Fuxing Road, Haidian District, Beijing, China

⁸Department of Orthopedic Surgery, The First Medical Center, Chinese PLA General Hospital, 28 Fuxing Road, Beijing, People's Republic of China

Received: 27 October 2023 / Accepted: 2 March 2024

Published online: 10 April 2024

References

1. Conaghan PG, Porcheret M, Kingsbury SR, et al. Impact and therapy of osteoarthritis: the Arthritis Care OA Nation 2012 survey. *Clin Rheumatol*. 2015;34:1581–8. <https://doi.org/10.1007/s10067-014-2692-1>.
2. Sasek C. An update on primary care management of knee osteoarthritis. *JAAPA*. 2015;28:37–43. <https://doi.org/10.1097/01.JAA.0000458853.38655.02>.
3. Simon S, Schwarz GM, Aichmair A, et al. Fully automated deep learning for knee alignment assessment in lower extremity radiographs: a cross-sectional diagnostic study. *Skeletal Radiol*. 2022;51:1249–59. <https://doi.org/10.1007/s00256-021-03948-9>.
4. Bouché P-A, Aubert T, Corsia S, et al. Systematic alignments yield balanced knees without additional releases in only 11% of knee arthroplasties: a prospective study. *Knee Surg Sports Traumatol Arthrosc*. 2022. <https://doi.org/10.1007/s00167-022-07252-4>.
5. Skyttä ET, Lohman M, Tallroth K, Remes V. Comparison of standard anteroposterior knee and hip-to-ankle radiographs in determining the lower limb and implant alignment after total knee arthroplasty. *Scand J Surg*. 2009;98:250–3. <https://doi.org/10.1177/145749690909800411>.
6. Langenbach MR, Dohle J, Zirngibl H. [Determination of the axis after totalendoprosthesis of the knee: functional X-ray photography as golden standard]. *Z Orthop Ihre Grenzgeb*. 2002;140:32–6. <https://doi.org/10.1055/s-2002-22088>.
7. Paley D, Herzenberg JE, Tetsworth K, et al. Deformity planning for frontal and sagittal plane corrective osteotomies. *Orthop Clin North Am*. 1994;25:425–65.
8. Rozzanigo U, Pizzoli A, Minari C, Caudana R. Alignment and articular orientation of lower limbs: manual vs computer-aided measurements on digital radiograms. *Radiol Med*. 2005;109:234–8.
9. Takahashi T, Yamanaka N, Komatsu M, et al. A new computer-assisted method for measuring the tibio-femoral angle in patients with osteoarthritis of the knee. *Osteoarthritis Cartilage*. 2004;12:256–9. <https://doi.org/10.1016/j.joca.2003.10.005>.
10. Sled EA, Sheehy LM, Felson DT, et al. Reliability of lower limb alignment measures using an established landmark-based method with a customized computer software program. *Rheumatol Int*. 2011;31:71–7. <https://doi.org/10.1007/s00296-009-1236-5>.
11. Zahn RK, Renner L, Perka C, Hommel H. Weight-bearing radiography depends on limb loading. *Knee Surg Sports Traumatol Arthrosc*. 2019;27:1470–6. <https://doi.org/10.1007/s00167-018-5056-6>.
12. Kannan A, Hawdon G, McMahon SJ. Effect of flexion and rotation on measures of coronal alignment after TKA. *J Knee Surg*. 2012;25:407–10. <https://doi.org/10.1055/s-0032-1313756>.
13. Maderbacher G, Baier C, Benditz A, et al. Presence of rotational errors in long leg radiographs after total knee arthroplasty and impact on measured lower limb and component alignment. *Int Orthop*. 2017;41:1553–60. <https://doi.org/10.1007/s00264-017-3408-3>.
14. Feldman DS, Henderson ER, Levine HB, et al. Interobserver and intraobserver reliability in lower-limb deformity correction measurements. *J Pediatr Orthop*. 2007;27:204–8. <https://doi.org/10.1097/01.bpb.0000242441.96434.6f>.
15. Akhmedov B, Sung KH, Chung CY, et al. Reliability of lower-limb alignment measurements in patients with multiple epiphyseal dysplasia. *Clin Orthop Relat Res*. 2012;470:3566–76. <https://doi.org/10.1007/s11999-012-2548-4>.
16. Pavlovic N, Harris IA, Boland R, et al. The effect of body mass index and preoperative weight loss in people with obesity on postoperative outcomes to 6 months following total hip or knee arthroplasty: a retrospective study. *Arthroplasty*. 2023;5:48. <https://doi.org/10.1186/s42836-023-00203-5>.
17. Bowman A, Shunmugam M, Watts AR, et al. Inter-observer and intra-observer reliability of mechanical axis alignment before and after total knee arthroplasty using long leg radiographs. *Knee*. 2016;23:203–8. <https://doi.org/10.1016/j.knee.2015.11.013>.
18. Finsterwald MA, Lu V, Andronic O, et al. Popliteal tendon impingement as a cause of pain following total knee arthroplasty: a systematic review. *Arthroplasty*. 2023;5:45. <https://doi.org/10.1186/s42836-023-00201-7>.
19. Cho BW, Lee T-H, Kim S, et al. Evaluation of the reliability of lower extremity alignment measurements using EOS imaging system while standing in an even weight-bearing posture. *Sci Rep*. 2021;11:22039. <https://doi.org/10.1038/s41598-021-01646-z>.
20. Tack A, Preim B, Zachow S. Fully automated Assessment of knee alignment from full-Leg X-Rays employing a YOLOv4 and Resnet Landmark regression Algorithm (YARLA): data from the Osteoarthritis Initiative. *Comput Methods Programs Biomed*. 2021;205:106080. <https://doi.org/10.1016/j.cmpb.2021.106080>.
21. Zhang Z, Huang C, Jiang Q, et al. Guidelines for the diagnosis and treatment of osteoarthritis in China (2019 edition). *Ann Transl Med*. 2020;8:1213. <https://doi.org/10.21037/atm-20-4665>.
22. Liu W, Wang Y, Jiang T, et al. Landmarks detection with anatomical constraints for total hip arthroplasty preoperative measurements. In: Martel AL, Abolmaesumi P, Stoyanov D, et al. editors. *Medical Image Computing and Computer assisted intervention – MICCAI 2020*. Cham: Springer International Publishing; 2020. pp. 670–9.
23. Sun K, Xiao B, Liu D, Wang J. (2019) Deep High-Resolution Representation Learning for Human Pose Estimation.
24. ImageNet Large Scale Visual Recognition Challenge | SpringerLink. <https://link.springer.com/article/10.1007/s11263-015-0816-y>. Accessed 6 Nov 2022.
25. Liu W, Anguelov D, Erhan D, et al. SSD: single shot MultiBox detector. In: Leibe B, Matas J, Sebe N, Welling M, editors. *Computer vision – ECCV 2016*. Cham: Springer International Publishing; 2016. pp. 21–37.
26. Kingma DP, Ba J. (2017) Adam: A Method for Stochastic Optimization.
27. Nguyen TP, Chae D-S, Park S-J, et al. Intelligent analysis of coronal alignment in lower limbs based on radiographic image with convolutional neural network. *Comput Biol Med*. 2020;120:103732. <https://doi.org/10.1016/j.combiomed.2020.103732>.
28. Ramazanian T, Yan S, Rouzrokh P, et al. Distribution and correlates of hip-knee-ankle Angle in early osteoarthritis and preoperative total knee arthroplasty patients. *J Arthroplasty*. 2022;37:170–S175. <https://doi.org/10.1016/j.arth.2021.12.009>.
29. Bayramoglu N, Nieminen MT, Saarakkala S. Automated detection of patellofemoral osteoarthritis from knee lateral view radiographs using deep learning: data from the Multicenter Osteoarthritis Study (MOST). *Osteoarthritis Cartilage*. 2021;29:1432–47. <https://doi.org/10.1016/j.joca.2021.06.011>.
30. Pei Y, Yang W, Wei S, et al. Automated measurement of hip-knee-ankle angle on the unilateral lower limb X-rays using deep learning. *Phys Eng Sci Med*. 2021;44:53–62. <https://doi.org/10.1007/s13246-020-00951-7>.

Publisher's Note

Springer Nature remains neutral with regard to jurisdictional claims in published maps and institutional affiliations.